# Controlling EMI with A Chaotic Peak Current-mode Boost Converter


H. Li, Z. Li and W.A. Halang
Faculty of Electrical and Computer Engineering
Fernuniversität in Hagen
58084 Hagen, Germany
Email: zhong.li@fernuni-hagen.de

Juan Gonzalo Barajas Ramirez
Division de Matematicas Aplicadas y Sistemas Computacionales -DMASC IPICyT



***Abstract*— In this paper, a novel boost converter is designed where its current mode control is dependent on two reference currents and an external clock. A detailed study on its dynamics is carried out based on its corresponding current mapping function. As demonstrated in both simulations and experiments, by operating the proposed boost converter in its chaotic mode, the electromagnetic interference can be reduced and the ripples of the converter's output are greatly suppressed.**


## I. Introduction

The dynamics of DC-DC converters, either boost or buck converters, have been extensively studied in the last few decades. The recent observation of chaotic dynamics in these converters, have also opened a new direction of research, while its distinct effect on reducing electromagnetic interference (EMI) has widely been reported [1] - [10].

The innovative work by Deane and Hamill [1] in 1996 may be the first design that utilized chaos for the improvement of the electromagnetic compatibility (EMC) of power supplies. Their idea was later reformulated in [2] and modified by applying some other control schemes [3]. From all the reported works, it can be concluded that EMC is effectively improved by the introduction of chaos via current mode control of a power converter.

In [4], a detailed study on the parametric design of a chaotic DC-DC converter was carried out based on its periodic spectral components. Similarly, but focusing on chaos control and utilization of chaos, design improvement were suggested in [5], while a low-EMI chaotic peak current-mode controlled boost converter was experimentally reported in [6].

However, despite of the success of EMI suppression using chaos, there are two opened problems to be tackled with. As observed in the previous designs, ripples of the output current are usually much greater than those operated in periodic mode [7]. Recognizing that a DC-DC converter is mainly used as a power supply of a system, large ripples simply imply a degradation of performance. Although an explicit relationship between ripples and spectral spreading of the current has been obtained in [11], it is still a difficult task to design a suitable control in order to suppress the ripples to a desirable level.

In addition, it is found that the power of the background spectra will also be increased, although the peak values of the power spectrum is reduced. This hence will result in a larger power consumption, becoming another major disadvantage of these designs.

It should be emphasized that these two disadvantages are also found in other chaotic power converters [8], [9], and in turns, seriously impeded their popularity. Therefore, it is the objective of this paper to address the questions of how to improve the control method for chaos-based DC-DC converters so that low EMI and small output ripples can be achieved, and to verify the relationship between the ripples and background spectrum.

The rest of the paper is organized as follows. In Sect. II, a new design of peak current-mode boost converter is proposed and its corresponding chaotic mapping function is derived. Based on the mapping function, the dynamical characteristics of the converter, including spectrum analysis, bifurcating and chaotic behaviors, are analyzed in Sect. III. Its performance in terms of EMI reduction and ripple suppression are also verified and demonstrated with simulation results in the same section. The design is then further confirmed based on the experiments described in Sect. IV. Finally, concluding remarks are given in Sect. V.

## II. A new design of current-mode boost converter

Figure 1 depicts a new design of current mode converter, which is considered as an enhanced version of that proposed in [4]. It consists of a current-mode boost converter (see Fig. 1 (a)), and a switch control generated by a simple circuit shown in Fig. 1 (b). In the followings, its dynamics will be studied, which contributes its attractive performance on EMI and ripple suppression.

Referring to Fig. 1 (b), the switch $S$ is now controlled by three elements, namely a clock with period $T_C$, a lower reference current signal $I_1$ and an upper one $I_2$.

Depending on the value of $T_C$, three different cases can be categoried:

Case I: $t_2 \geq T_C$,
Case II: $T_A \geq T_C > t_2$, and
Case III: $T_C \geq T_A$,

where $t_1$ is the rising time of $i(t)$ from $I_1$ to $I_2$, $t_2$ is the falling time of $i(t)$ from $I_2$ to $I_1$, and $T_A = t_1 + t_2$.

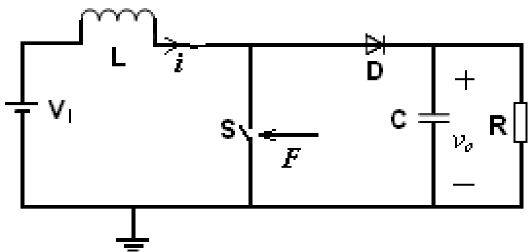


(a)

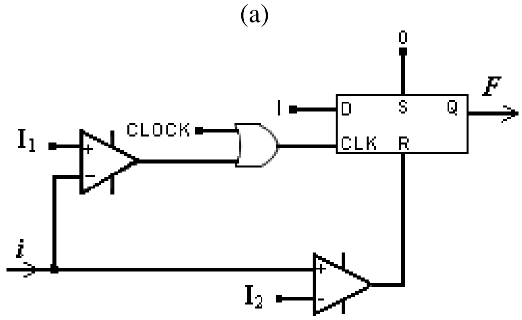


(b)

Fig. 1. (a) Current-mode boost converter (b) Switch control

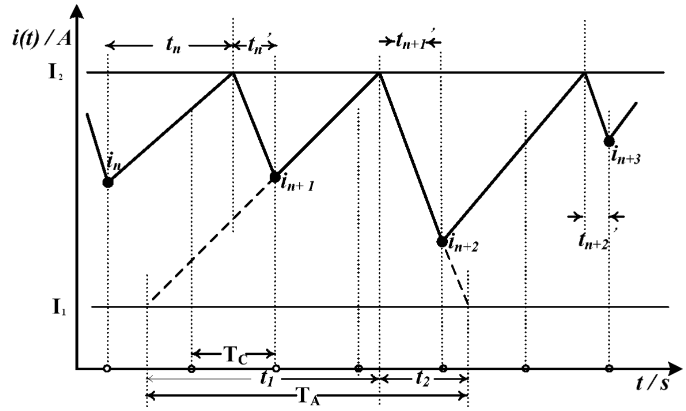


(a) Case I: $t_2 \geq T_C$

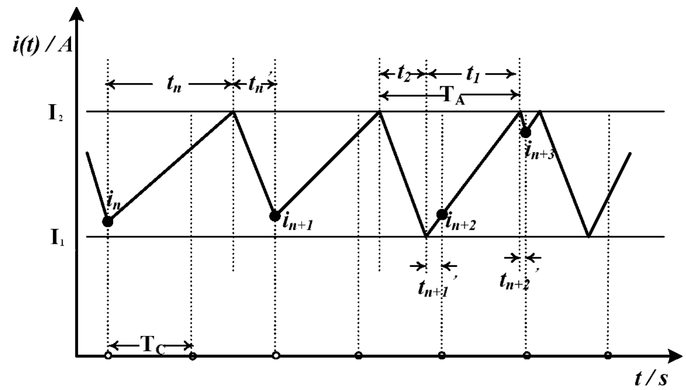


(b) Case II: $T_A \geq T_C > t_2$

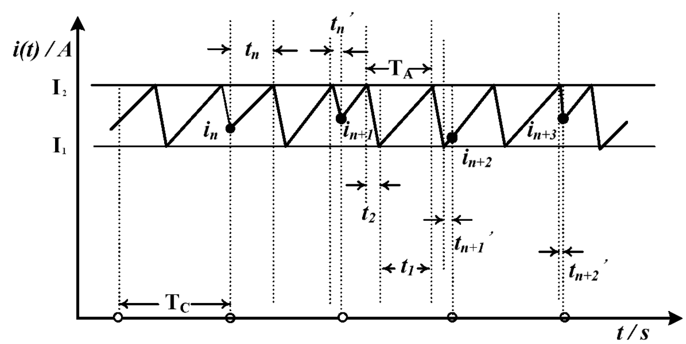


(c) Case III: $T_C \geq T_A$

Fig. 2. Different current waveforms $i(t)$ obtained from the boost converter

For each case, the corresponding inductor current waveforms can be obtained as shown in Fig. 2.

According to Fig. 2, $i_n$ is only sampled at the moment when S opens in Case I, however, there appears a new kind of $i_n$ for Cases II and III which can be sampled at the some clock cycles even when S is closed.

Similar to [4], the analysis of the proposed converter is carried out based on a discrete-time mapping of $i(t)$. Let $i_n$ be the inductor current sampled at the instants of the clock pulses as $i(t)$ is decreasing, and we will focus on the time interval when $i(t)$ changes from $i_n$ to $i_{n+1}$. For clarity, a time mapping is assumed, such that $i(\tau_n) = i_n$ when $\tau_n = 0$. Referring to Fig. 2, $S$ is closed at $\tau_n = 0$, and hence

$$\begin{cases} \frac{di}{d\tau_n} = \frac{V_I}{L}, \\ i(\tau_n) = i_n + \frac{V_I}{L}\tau_n, \end{cases} \tag{1}$$

where $V_I$ is input voltage and $L$ is the inductance.

Let $t_n$ be the time required for the current from $i_n$ to reach $I_2$. Based on (1), we have

$$t_n = \frac{(I_2 - i_n)L}{V_I}. \tag{2}$$

The switch $S$ is then opened and $i(\tau_n)$ is governed by

$$\frac{di}{d\tau_n} = \frac{(V_I - \overline{V}_O)}{L}, \tag{3}$$

where $\overline{V}_O$ is the mean output voltage. Therefore,

$$i(\tau_n) = I_2 + \frac{V_I - \overline{V}_O}{L}(\tau_n - t_n) \tag{4}$$

until the next clock pulse arrives or $i(\tau_n) = I_1$.

The mean output voltage $\overline{V}_O$ can then be approximated by equating the mean of the aperiodic inductor current with a periodic one. Therefore, one obtains the following input-output relationship:

$$\overline{V}_O^3 + \overline{V}_O(\frac{V_I T_p}{2L} - I_2)RV_I - R\frac{T_p V_I^3}{2L} = 0. \tag{5}$$

In [4], $T_p$ is set to be $T_C$. However, in our Cases II and III, $T_p$ is also dependent on $I_2$ and $I_1$. As shown in Fig. 2, $T_p$ is proportional to $I_2$ but inversely proportional to $I_1$. Therefore, $T_p$ can be determined as:

$$T_p = \left(a\frac{I_2}{I_1} + b\right)T_C, \tag{6}$$

using first order approximation and $a$ and $b$ are some constants.

According to our experimental results, it is found that $a = 2.0499$ and $b = 1.5455$, while the relative errors of $\overline{V}_O$ are well within 2%, much better than reported in [4].

Let $t_n^{'}$ be the time interval from the last action of $S$ within a clock period to the next clock pulse, it can be derived that

$$t_n^{'} = \begin{cases} \varepsilon & \text{if} \quad \varepsilon \leq t_2, \\ \varepsilon - t_2 & \text{otherwise}, \end{cases} \tag{7}$$

where $\varepsilon = [T_C - (t_n \mod T_C)] \mod T_A$.

Referring to Fig. 2, one has

$$i_{n+1} = \begin{cases} I_2 + \frac{(V_I - \overline{V}_O)}{L}\varepsilon & \text{if} \quad \varepsilon \leq t_2, \\ I_1 + \frac{V_I}{L}(\varepsilon - t_2) & \text{otherwise}. \end{cases} \tag{8}$$

Defining

$$x_n = \frac{t_n}{T_C} = \frac{(I_2 - i_n)L}{V_I T_C} \quad \text{and} \quad \alpha = \frac{\overline{V}_O}{V_I} - 1,$$

based on (8) a discrete mapping can be constructed as

$$x_{n+1} = \begin{cases} \alpha x_n', & \text{if} \quad x_n' \leq \gamma, \\ \rho + \gamma - x_n', & \text{otherwise}, \end{cases} \tag{9}$$

where

$$\begin{aligned} x_n' &= \beta\{[\frac{1}{\beta}(1 - (x_n \mod 1))] \mod 1\}, \\ \gamma &= \frac{t_2}{T_C}, \quad \beta = \frac{T_A}{T_C} \quad \text{and} \quad \rho = \frac{(I_2 - I_1)L}{V_I T_C}. \end{aligned}$$

It is remarked that, for Case I or $t_2 > T_C$, (9) becomes

$$x_{n+1} = \alpha\left[1 - (x_n \mod 1)\right],$$

which is equivalent to the chaotic mapping obtained in [4], and hence can be considered as a special case for the proposed design.

## III. Characteristics of the Current Mapping Function

The characteristics of the mapping function (9) are to be studied, while their dependence on $I_1$ is focused. Referring to Fig. 1, it is assumed that that $V_I = 10V$, $L = 1mH$, $C = 12\mu F$, $T_C = 100\mu s$, and $R = 30\Omega$, onwards.

### A. Spectrum analysis

The three possible cases given in Sect. II are investigated. Figures 3, 4 and 5 show the time evolutions of the inductor currents $i(t)$, the phase portrait of $i_n$ against $i_{n+1}$ and the corresponding spectra of each case, base on $I_1 = 1A$, $2.25A$, and $3.7A$, respectively and $I_2 = 4A$.

Comparing the waveforms in Figs. 3 (a), 4 (a) and 5 (a), it is noticed that the ripples of $i(t)$ can greatly be reduced when a larger $I_1$ is applied. On the other hand, as indicated by the corresponding phase portraits and the power spectrum, a complicate dynamics are obesrved. The power is well spread over the entire frequency band, while it is interesting to notice that, instead of having a maximum peak of a magnitude close to the clock frequency $T_C$ as in Cases I and II, the peak is shifted to a frequency of approximately $\frac{1}{T_A}$ =23.5 KHz in Case III.

In all cases, the low frequency components of $i(t)$ are suppressed and a better spectrum distribution is obtained. However, it is also noticed that the background spectrum is not significantly improved, even though the ripples are suppressed.

### B. Bifurcation and the Lyapunov exponents

As indicated by the broadband spectrum obtained in the previous section, the boost converter (9) possesses an interesting chaotic nature. In the sequel, this nature is further investigated based on its bifurcation diagrams and Lyapunov exponents.

Figure 6 depicts the bifurcation diagram of $x_n$ versus $I_1$, and the corresponding maximum Lyapunov exponents (LEs). The existence of positive LEs confirms the chaotic mode of the system and some periodic windows are also noticed in between. It can be explained by the fact that (9) can be

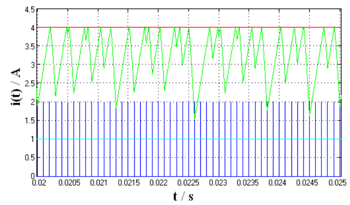


(a) $i(t)$

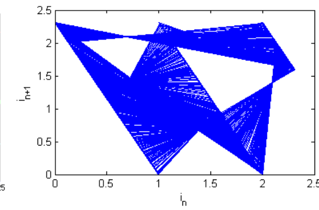

(b) Phase portrait $i_n$ vs $i_{n+1}$

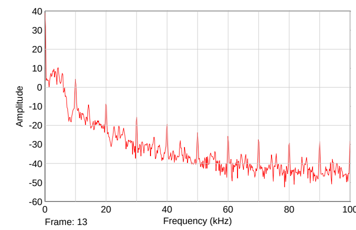


(c) Spectrum of (a)

Fig. 3. Case I: $t_2 \geq T_C$

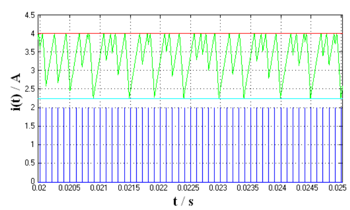


(a) $i(t)$

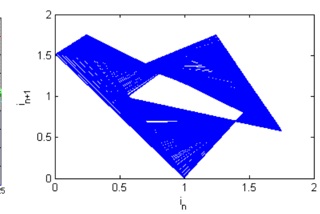

(b) Phase portrait $i_n$ vs $i_{n+1}$

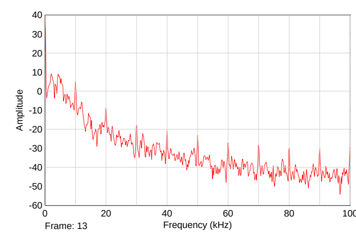


(c) Spectrum of (a)

Fig. 4. Case II: $T_A \geq T_C > t_2$

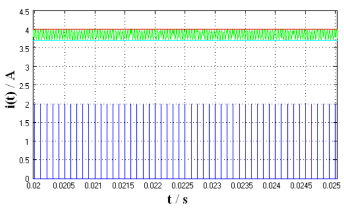


(a) $i(t)$

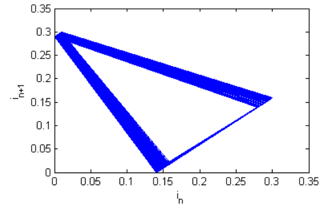


(b) Phase portrait $i_n$ vs $i_{n+1}$

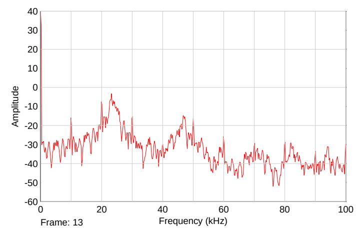


(c) Spectrum of (a)

Fig. 5. Case III: $T_C \geq T_A$

rewritten as $x_{n+1} = \beta(1 - \frac{1}{\beta}x'_n)$ when $\rho + \gamma = \beta$, giving $LE = 0$ and hence the system is in a periodic mode.

Similarly, the bifurcation diagrams of $x_n$ versus $V_I$ and $x_n$ versus $T_C$ are obtained and shown in Figs. 7 and 8. It is remarked that Case III (it is also our main interest) is assumed.

In Fig. 7, a route from period to chaos is clearly observed when the input voltage $V_I$ is decreased, while some periodic windows exist. Similar conclusion is drawn from the bifurcation diagram given in Fig. 8. Therefore, the mapping (9) exhibits rich dynamical behavior like bifurcation and chaos, which constitutes the corner stone of our design to reduce EMI and improve EMC.

## C. EMC performance

In order to design a good DC/DC converter, its EMC performance is critical. As shown in the bifurcation diagram obtained in the previous section, the proposed converter operates either in chaotic or periodic mode. In the followings, simulations are conducted to compare which operating mode will provide better EMI suppression.

Figure 9 (a)–(c) depict the spectra when the boost converter operates in chaotic modes with $I_1 = 0A,\ 2.42A$, and $3.1A$ ($I_2 = 4A$) for the three specified cases. A smaller maximum peak value is obtained when $I_1 = 3.1A$, as compared with the case of $I_1 = 0A$ (Note: $I_1 = 0A$ is equivalent to the original design given in [4]), and a slight shift of the dominant frequency is observed.

For periodic cases, the the power spectra of the corresponding inductor currents with $I_1 = 1.979A,\ 2.62A$, and $2.958A$ ($I_2 = 4A$) are shown in Fig. 9 (d)–(f). The peak amplitude remains the same with the base frequency shifting to higher frequencies when $I_1$ is increased (Note: an increase of $I_1$ results in a decrease of ripple amplitudes).

Therefore, by operating the designed converter in chaotic mode, the switch control strategy in Fig. 1 (b) not only suppresses the ripples, but also improves EMC.

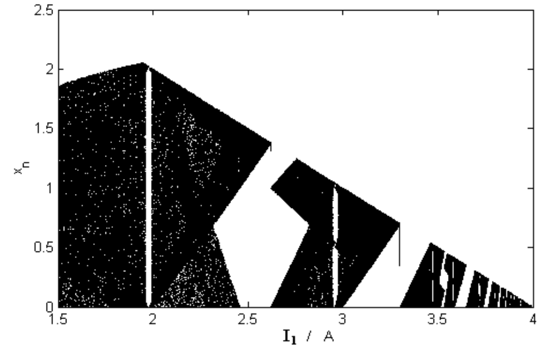


(a) Bifurcation of $x_n$ vs $I_1$

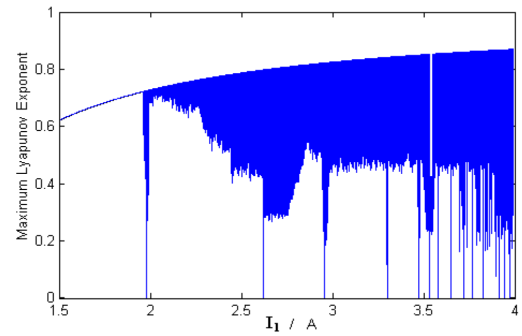


(b) Maximum LE

Fig. 6. Bifurcation of $x_n$ against $I_1$ and the corresponding maximum LE

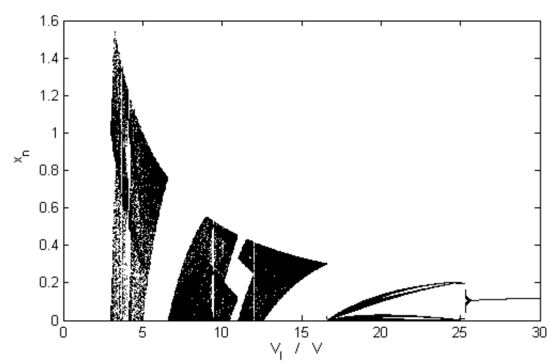


(a) Bifurcation of $x_n$ vs $V_I$

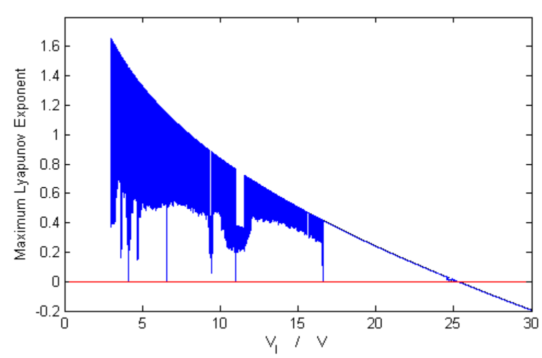


(b) Maximum LE

Fig. 7. Bifurcation of $x_n$ against $V_I$ and the corresponding maximum LE

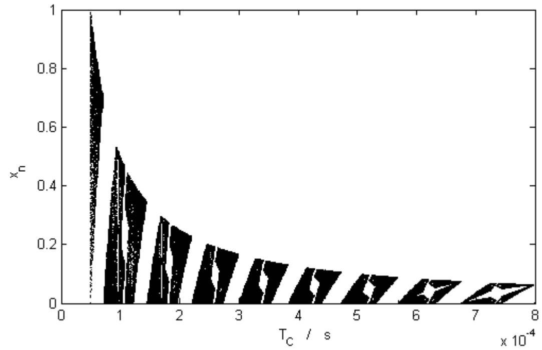


(a) Bifurcation of $x_n$ vs $T_C$

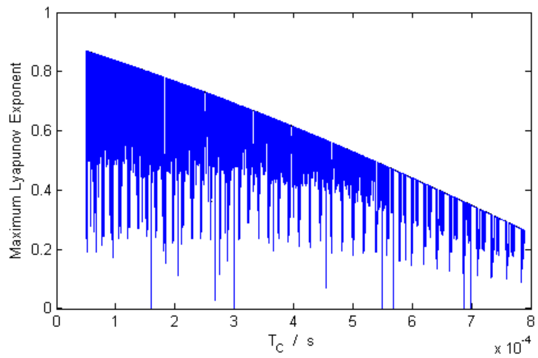


(b) Maximum LE

Fig. 8. Bifurcation of $x_n$ against $T_C$ and the corresponding maximum LE

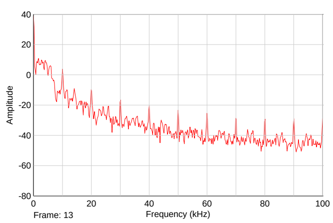


(a) $I_1 = 0A$

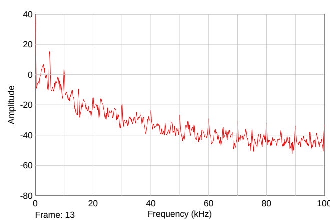


(b) $I_1 = 2.42A$

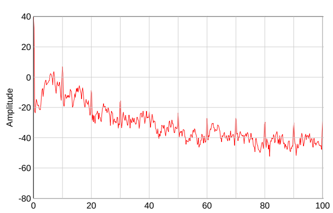


(c) $I_1 = 3.1A$

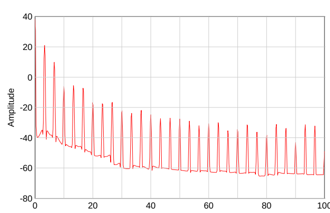


(d) $I_1 = 1.979A$

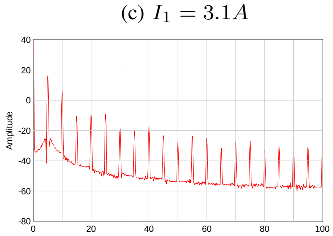


(e) $I_1 = 2.62A$

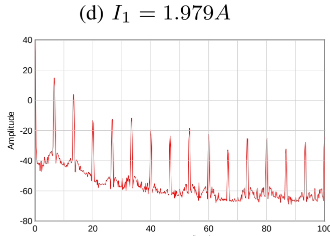


(f) $I_1 = 2.958A$

Fig. 9. Spectra with different $I_1$: (a)–(c) chaotic mode and (d)–(e) periodic mode

## IV. Experimental verification

The design in Fig. 1 is realized with discrete components, while the major components are tabulated in Table I. In addition, it is set that $V_I = 10V$, $T_C = 100\mu s$, $L = 0.56mH$, $C = 47\mu F$, and $R = 30\Omega$.

TABLE I
THE LIST OF MAIN COMPONENTS

| Component | Device |
|---|---|
| diode | MBR2045CT |
| switch | IRFZ234N |
| current sensor | LA-55-P |
| flip-flop | 74HC74N |
| comparator | LM393 |
| driver | 34152P |

Figures 10 (a), (c) and (e) show the current waveforms for the three cases with the boost converter operating in periodic mode with the corresponding spectra given in Figs. 10 (b), (d) and (f). As compared with the simulations presented in Sect. III-C, a close match is confirmed. The maximum peak of the frequency are also unchanged, even though the ripples have been greatly reduced (the peak-to-peak ripples are $2.4A$, $1.4A$, and $0.9A$, respectively).

When the boost converter is operated in chaotic mode, as shown in Fig. 11, an improvement of EMI suppression is clearly demonstrated with an increase of $I_1$, while a large reduction of ripples can be achieved at the same time. It should be emphasized that $I_1 = 0A$ is equivalent for the design presented in [4]. The experimental results are also consistent to the observations in Sect. III-A and no obvious relationship between the ripple magnitude and the background spectrum is found.

## V. Conclusion

In this paper, a new peak current-mode boost converter is proposed and studied. The current control is dependent on two reference currents and an external clock, which can be realized in a simple circuit.

By deriving its current mapping function, it is found that the boost converter can exhibit complicated dynamics. Bifurcations and chaotic dynamics are easily obtained by the introducton of $I_1$ as compared with the design given in [4].

The performance of the proposed design is confirmed both in simulations and experiments, and it shows that the current ripples and also the EMI are suppresseed. It is also noticed that there is a shift of the dominant frequencies in the power spectrum when $I_1$ is increased, for which further studies will be carried out for identifying the causes.

## References

[1] J.H.B. Deane, D.C. Hamill, "Improvement of power supply EMC by chaos", *Electronics Letters*, vol. 32, no. 12, pp. 1045, 1996.

[2] D.C. Hamill, J.H.B. Deane, and P.J. Aston, "Some applications of chaos in power converters", *IEE Colloquium on New Power Electronic Techniques (Digest No: 1997/091)*, pp. 5/1–5/5, May 1997.

[3] A. Grial, A. EI Aroudi, L. Martinez-Salamero, R. Leyva and J. Maixe, "Current control technique for improving EMC in power converters", *Electronics Letters*, vol. 37, no. 5, pp. 274–275, March 2001.

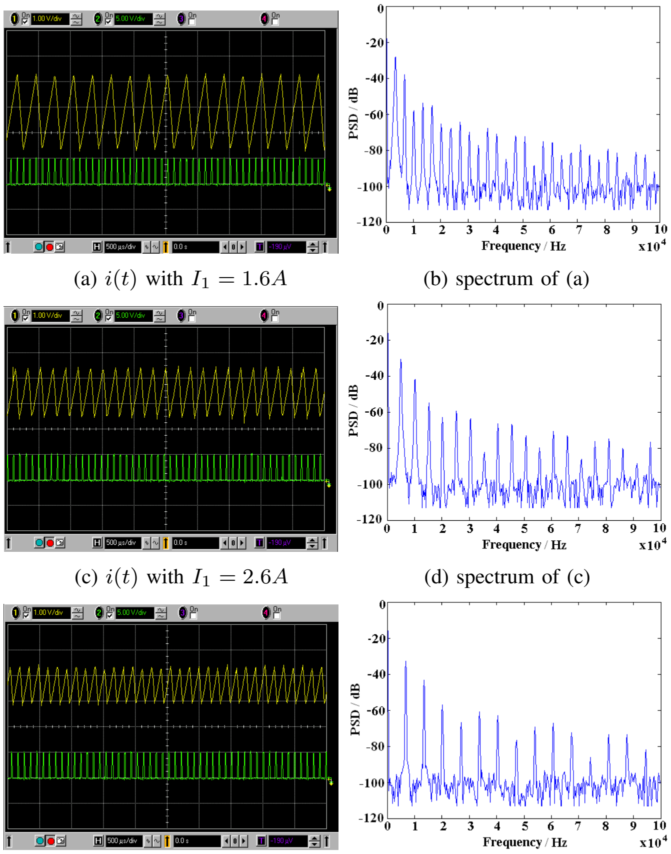


(a) $i(t)$ with $I_1 = 1.6A$ (b) spectrum of (a)

(c) $i(t)$ with $I_1 = 2.6A$ (d) spectrum of (c)

(e) $i(t)$ with $I_1 = 3.1A$ (f) spectrum of (e)

Fig. 10. Current waveforms and corresponding spectra in periodic mode for Cases I–III

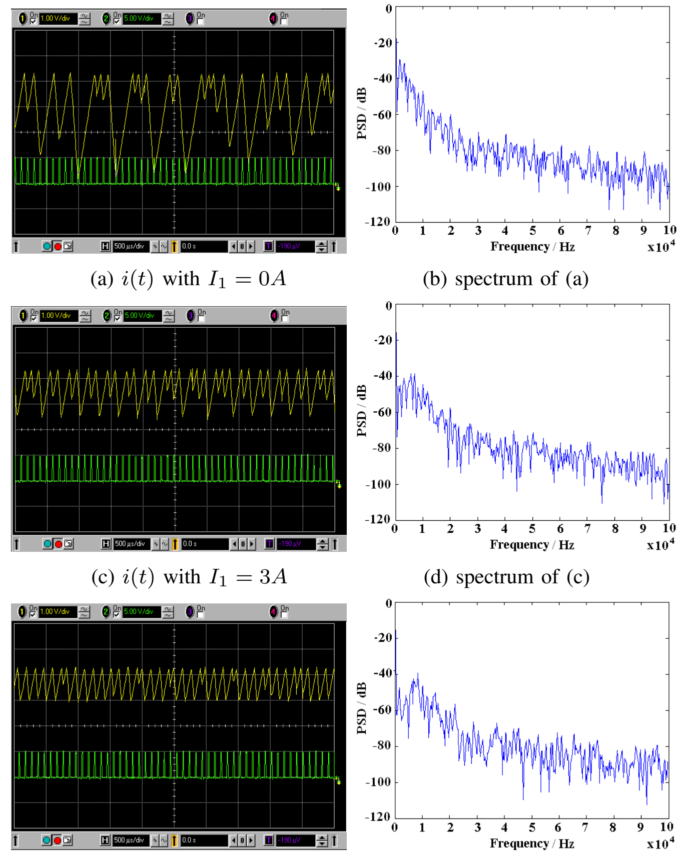


(a) $i(t)$ with $I_1 = 0A$ (b) spectrum of (a)

(c) $i(t)$ with $I_1 = 3A$ (d) spectrum of (c)

(e) $i(t)$ with $I_1 = 3.2A$ (f) spectrum of (e)

Fig. 11. Current waveforms and corresponding spectra in chaotic mode for Cases I–III


[4] J.H.B. Deane, P. Ashwin, D.C. Hamill and D.J. Jefferies, "Calculation of the periodic spectral components in a chaotic DC-DC converter", *IEEE Transactions on Circuits and Systems I*, vol. 46, no. 11, pp. 1313–1319, 1999.

[5] A.L. Baranovski, A. Mogel, W. Schwarz and O. Woywode, "Chaotic control of a DC-DC converter", *IEEE Int. Symp. Circuits and Systems*, pp. II/108-II/111, May 2000.

[6] M. Balestra, M. Lazzarini, G. Setti, and R. Rovatti, "Experimental performance evaluation of a low-EMI chaos-based current-programmed DC-DC Boost converter", *IEEE Int. Symp. Circuits and Systems*, vol. 2, pp. 1489–1492, May 2005.

[7] S. Banerjee, D. Kastha and S. SenGupta, "Minimising EMI problems with chaos", *Int. Conf. Electromagnetic Interference and Compatibility*, pp. 162–167, Feburay 2002.

[8] R. Mukherjee, S. Nandi and S. Banerjee, "Reduction in spectral peaks of DC-DC converters Using chaos-modulated clock", *IEEE Int. Symp. Circuits and Systems*, vol. 4, pp. 3367–3370, May 2005.

[9] R. Yang, B. Zhang, F. Li, and J.J. Jiang, "Experiment research of chaotic PWM suppressing EMI in converter", *IEEE 5th Int. Conf. Power Electronics and Motion Control*, vol. 1, pp.1–5, August 2006.

[10] S. Banerjee, A.L. Baranovski, J.L.R. Marrero, and O. Woywode, "Minimizing electromagnetic interference problems with chaos", *IEICE Trans. Fundamentals*, vol. E87-A, no. 8, pp. 2100–2109, 2004.

[11] A.L. Baranovski, H. Gueldner, W. Schwarz, J. Weber and O. Woywode, "On the trade-off of ripple and spectral properties of chaotic DC-DC converters", *Int. Symp. Nonlinear Theory and Its Applications*, October 2002.


## BIOGRAPHIES

**Hong Li** received her BS and MS from Taiyuan University of Technology and South China University of Technology, in 2002 and 2005, respectively. She is now a Ph.D. student at the FernUniversitaet in Hagen, Germany. Her research interests include power electronics, electromagnetic interference and chaos control and its applications.

**Zhong Li** received his BS, MS and Ph.D. from Sichuan University, Jinan University, and South China University of Technology, in 1989, 1996, and 2000, respectively. He is now a junior professor at the FernUniversitaet in Hagen, Germany. His research interests include chaos theory and chaos control, application of chaos in cryptography, fuzzy control and its applications, and coordinated control of networked multi-agent systems

**Wolfgang A. Halang**, born 1951 in Essen, Germany, received a doctorate in mathematics from Ruhr-Universität Bochum in 1976, and a second one in computer science from Universität Dortmund in 1980. Since 1992 he holds the Chair of Computer Engineering in the Faculty of Electrical and Computer Engineering at Fernuniversität in Hagen, Germany. His research interests comprise all major areas of hard real-time computing with special emphasis on safety-related systems.

**Dr. Barajas Ramíez** graduated in 1995, with the degree Ingeniero Industrial en Electrónica (Industrial Engineering majoring in Electronics) from the Instituto Tecnológico de Tijuana. In 1997 he received the degree of Maestro en Ciencias en Electrónica y Telecomunicaciones con especialidad en Instrumentación y Control (Masters in Science, Electronics and Telecommunications, majoring in Instrumentation and Control) from CICESE in Ensenada México. In 2002, received the Doctor of Philosophy on Electrical Engineering degree from the University of Houston. Since 2004 he is a member of the National System of Researchers (SNI) of México, currently SNI-1.